Nikola Fischer, Paul Scheikl, Christian Marzi, Barbara Galindo-Blanco, Anna Kisilenko, Beat P. Müller-Stich, Martin Wagner, and Franziska Mathis-Ullrich*

Flexible Facile Tactile Sensor for Smart Vessel Phantoms

Abstract: Smart medical phantoms for training and evaluation of endovascular procedures ought to measure impact forces on the vessel walls worth protecting to provide feedback to clinicians and articulated soft robots. Recent commercial smart phantoms are expensive, usually not customizable to different applications and lack accessibility for integrated development. This work investigates piezoresistive films as highly integratable flexible sensors to be used in arbitrary soft vessel phantom anatomies over large surfaces and curved shapes providing quantitative measurement in the force range up to 1 N with 0.1 N resolution. First results show promising performance at the point of calibration and in a 5 mm range around it, with absolute measuring error of 28 mN and a standard deviation of ±10 mN and response times <500 ms. Future work shall address the optimization of response time and sensor shapes as well as the evaluation with experienced clinicians.

Keywords: force sensing, smart phantom, tactile sensor

https://doi.org/10.1515/cdbme-2021-1019

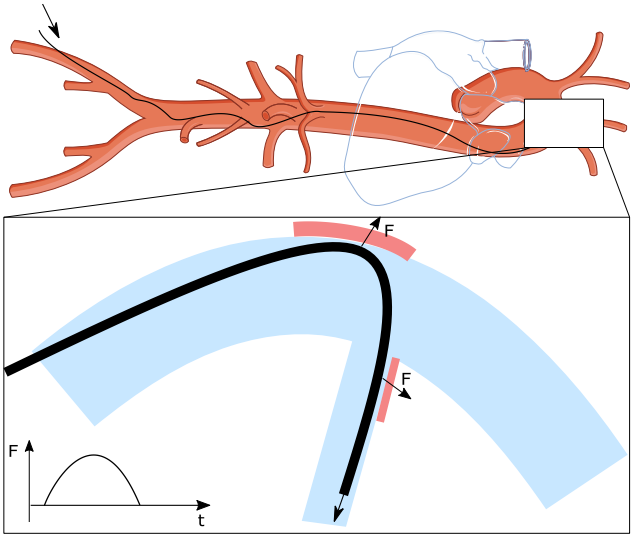

Figure 1: Schematic concept of a force-sensing smart vessel phantom (aorta with main branches) for use in training vascular surgeons and medical robotic systems. Aorta by SERVIER under CC BY 3.0.

1 Introduction

The clinical relevance of endovascular interventions steadily increases as vascular diseases continue to be one major contributor to death in developed countries [1]. However, they come at the cost of complex control of catheter devices that is mentally taxing for the surgeon and requires years of intensive practice. Mazomenos *et al.* argue in [2], that protecting the vessel wall is thereby one of the most essential skills for a novice clinician to train as excessive force on the vessels may lead to bleeding caused by ruptures in the vascular walls. Novel articulated soft robots and autonomous control thereof hold the potential to assist surgeons during such critical endovascular interventions through simplified control and automated navigation from preoperative information as by Karstensen *et al.* [3]. Here, a guidewire is manipulated by a trained neural network with two degrees of freedom inside a rigid 2D vessel phantom filled with blood-mimicking fluid made of glycerin and water. Moreover, endovascular robots may reduce radiation exposure to medical personnel. The preclinical development of soft articulated robots for endovascular interventions, however, depends on the availability of so-called ‘smart phantoms’ that are able to locate and quantify the forces that are exerted on the vascular walls by the robot for excessive testing to obtain a high safety level of the robotic system prior to clinical translation. Smart phantoms may further be used during surgical training and provide feedback to surgical novices. Thus, basic skills and understanding can be learned already before entering the

Nikola Fischer, Paul Scheikl, Christian Marzi, Barbara Galindo-Blanco, Franziska Mathis-Ullrich*: Health Robotics and Automation, Institute for Anthropomatics and Robotics, Karlsruhe Institute of Technology, 76131 Karlsruhe, Germany, e-mail: franziska.ullrich@kit.edu
Anna Kisilenko, Beat P. Müller-Stich, Martin Wagner: Department for General, Visceral and Transplantation Surgery, Heidelberg University Hospital, 69120 Heidelberg, Germany

operation room. Commercial smart vessel phantoms, especially virtual reality (VR) simulator systems, demonstrate sophisticated features, such as *CathLab VR* (CAE Healthcare, Canada), *Angio Mentor* (Simbionix USA Corp, USA), *VIST* (Mentics AB, Sweden), and the *CATHiS* (CATHI GmbH, Germany). These surgical trainers are able to measure collision and frictional forces during the intervention with real-time feedback for the trainee [4]. To increase authenticity, the *Endovascular Evaluator EVE* (BR Biomedical (P) Ltd., India) utilizes silicone with artery-like elasticity and friction coefficients to mimic the haptic experience of a real procedure in the operation room. However, those systems are often expensive and pose a financial hurdle for researchers and developers [4], [5]. Furthermore, they seldom provide the physical accessibility for robotic platforms or an API (Application Programming Interface) that exposes sensor data for integrated development.

We argue, that the scientific community would benefit from an affordable and facile contact force sensor for hard and soft phantoms that serve as testbeds for the development of novel articulated soft robots and to estimate applied forces during surgical training within those phantoms. Therefore, we propose a facile open source force sensor that can be integrated into various types of customized phantoms to mimic an individual patient's anatomy and provide force-sensing abilities for a specific medical procedure. The phantom is therefore equipped with a flexible and scalable sensor system that can be integrated at multiple arbitrary sections of interest. There, it can provide real-time data of the contact forces applied to the inner walls to provide an immediate user feedback and thereby an ideal testing environment for robotic systems or during training.

2 Material and Methods

2.1 Measuring Principle

Potential sensing principles for force impact sensing on flexible vessel walls include capacitive, piezoelectric, piezoresistive, and optoelectronic approaches. In particular, piezoresistive sensors using thin conductive films allow for subsequent addition of susceptibility to previously passive medical phantoms and their complex structure. Similar polymeric films such as the commercially available *Velostat* (i.e. linqustat, 3M Company, USA) have been used as smart material that changes its resistance when stretched to sensorize gloves for finger-gesture recognition [6], to develop a foot controller for navigation in VR [7], to measure body pressures with a wearable device [8], and to analyze sitting postures [9]. Despite the smaller sensitivity compared to other piezoresistive materials for sensing on flexible surfaces (piezoresistive ink by Voltec Electrónica, Columbia; *ThruMode* Matrix Arrayby Sensitronics, USA), *Velostat* offers low hysteresis [10]. Hopkins *et al.* [11] investigate *Velostat* and its performance characteristics when used in lower limb prostheses and found this inexpensive material easy to integrate to the individual stump interface although pointing out inaccuracy as a drawback. Thus, compared to commercially available piezoresistive and piezoelectric sensors with small thickness, *Velostat* appears to be a facile and cost-effective choice to sensorize large surfaces detecting static and dynamic impacts. At the same time, the material requires a relatively simple sensor setup compared to capacitive and optical sensing techniques. Its ability to be formed into an arbitrary shape makes it especially useful for application on irregular and organic structures such as vessel phantoms. Therefore, in this work *Velostat* was chosen as sensing material to cover a force sensing range up to 1 N.

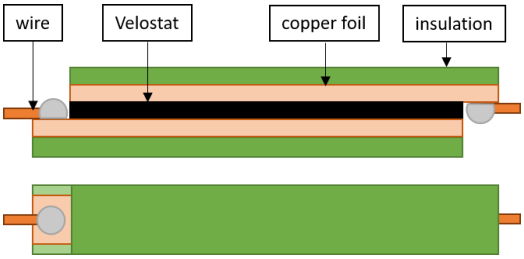

Figure 2: Lateral and top view schematic of the multi-layer sensor design including *Velostat*, copper foil and insulation.

2.2 Sensor Fabrication

Each sensor has dimensions of 100 mm × 16 mm and consists of a 100 µm thick layer of the piezoresistive material that is sandwiched between two 66 µm thick copper foil layers with conductive adhesive (3M Copper Foil Tape 1181, 3M Company, USA). Adhesive insulating foil (60 µm thick) is utilized for insulation, as illustrated in Figure 2.

2.3 Circuit Design

The smart material *Velostat* is a piezoresistive material that changes its electric resistance R_{sens} when physically stretched by normal and lateral stress induction, e.g. when a force is applied. The resistance R_{sens} of piezoresistive materials between two electrodes is inversely related to the applied normal force F as discussed in [12]

$$\boldsymbol{R_{\text{sens}} \propto \frac{\rho \cdot K}{F}} \tag{1}$$

where ρ is the resistance of the contacting surfaces and K is a function of the roughness and elastic properties of the surfaces. The resistance variation ΔR_{sens} is converted into a voltage variation ΔU_{sens} using a voltage divider and a signal amplifier (Texas Instruments MCP602, USA). The voltage at the flexible sensor may be obtained as in [10] by

$$\boldsymbol{U_{\text{sens}} = U_{\text{in}} \left(\frac{\rho \cdot K}{(F \cdot R_{\text{stat}}) + (\rho \cdot K)} \right)}. \tag{2}$$

Input voltage U_{in} and resistor R_{stat} were set to 15 V and 20 kΩ, respectively, to obtain a high sensitivity, i.e. a small force impact F leads to increased change of sensor voltage U_{sens}.

2.4 Signal Processing

Objective of the signal processing is to estimate applied forces on the sensor from the voltage characteristic in real-time. The signal processing steps are presented in Figure 3. First, U_{sens} as raw sensor signal is input as an analog signal to a micro controller (*Arduino UNO*) and converted into a digital signal with a sample time of 20 ms. The signal is smoothed using a convolution filter of rectangular shape and a sample length of 35 to reduce the noise. This length was derived experimentally as a suitable trade-off between the smoothness of the filtered data and the resulting delay that is directly dependent on the window length. The system uses two threshold values to determine the presence or absence of an impact. When the signal falls below U_{TH1}, a force is considered to be acting upon the system (excited-state). Threshold U_{TH2} is used to determine when the force is not applied anymore, such that the system evolves from excited-state to steady-state (Figure 3a). Calibrating U_{TH1} and U_{TH2} such that $U_{\text{TH2}} = U_{\text{TH1}} + \Delta$, where $\Delta > 0$, reduces noise and false positives. The thresholds were determined experimentally to allow for detection of 10 g increments and thus set to $U_{\text{TH1}} = -50$ mV and $U_{\text{TH2}} = -25$ mV corresponding approximately to 5 g and 2.5 g, respectively. When in excited-state, the signal's derivative is computed to reduce the response time between the impact of the force and the determination of its value (Figure 3b). Its local minimum is distinctive for the impact. A linear regression allows to determine a value for the impact weight (Figure 4) and the corresponding force F with the gravitational constant $g = 9.81\ \text{m/s}^2$.

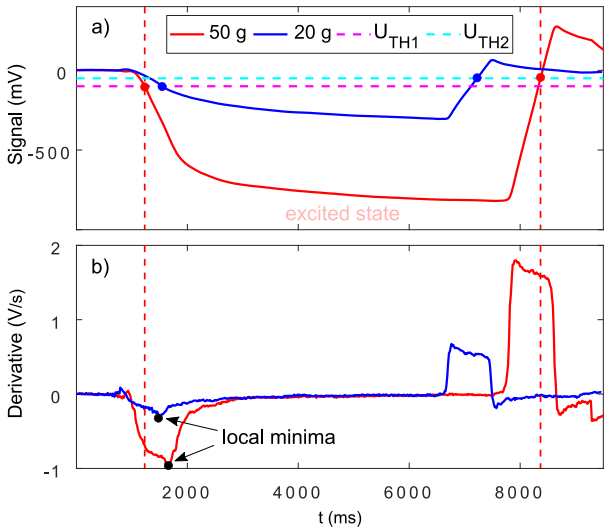

Figure 3: Signal processing: a) Smoothed sensor signal is monitored (steady-state) and the excited state is introduced when it falls below U_{TH1}; b) in excited state, the local minimum of the signal's time-derivative is obtained.

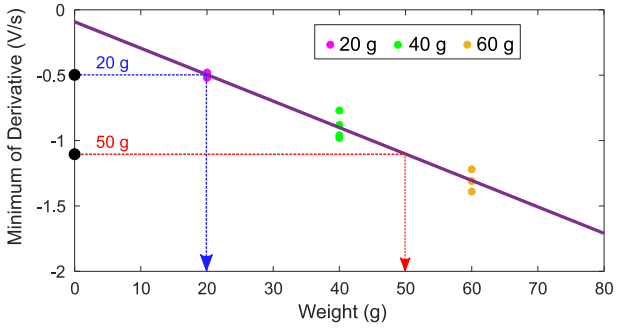

Figure 4: Linear interpolation for minima of impact-derivatives (20 g, 40 g and 60 g). For example, minimum-derivatives of 20 g and 50 g and corresponding weight impacts are indicated.

2.5 Sensor Integration

Figure 5 shows a schematic of the proof-of-concept proto type for sensor integration with a semi-open 2 mm thick vessel wall, 30 mm in diameter, from platinum-catalyzed elastomer, namely silicone rubber (Ecoflex 00-50, Smooth- On Inc., USA) and a 3D-printed curved

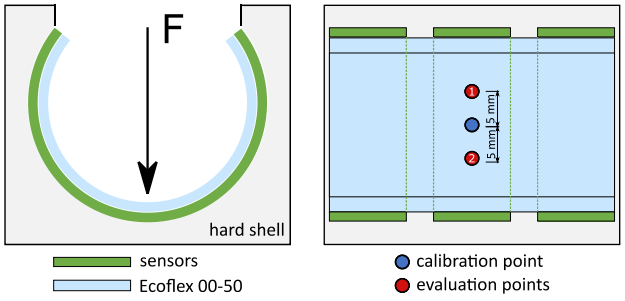

Figure 5: Schematic of sensor integration into the smart phantom and calibration/evaluation approach using gauged weights. Blue and red markers indicate impact location for the calibration and evaluation respectively. Lateral view: left, top view: right.

shell (printed on a *German RepRap X350pro*, Germany) from ABS filament (*TitanX*, FormFutura, Netherlands). The shell also serves as a rigid holder to mount the vessel in a predefined pose. Wires and terminals are included for easy electronic connection to the remaining electric circuit and micro controller. The semi-open design of the vessel phantom allows access to calibrate the sensor and evaluate the system before transferring it to more complex, closed vessel shapes. By aligning several sensor strips, contact forces can be spatially resolved along a vessel section.

2.6 Sensor Calibration

After installation of the sensor in a vessel phantom wall segment, the sensor system is calibrated to calculate the parameters of the linear least squares regression of the signal processing pipeline, namely the inclination and interception. These values are derived from linear interpolation between known impact-derivative values for (20 g, 40 g, and 60 g) at designated calibration points along the central longitudinal axis of the phantom (Figure 5). The impact force from the weights is transmitted via a 3D-printed plate with a cylindrical mandrel with 5 mm in diameter for a single-point impact similar to endovascular devices (Figure 6). An inclination of the calibration device allows to apply normal force impacts also to non-horizontal sections of the vessel circumference.

2.7 Sensor Evaluation

Measuring accuracy of the sensor was evaluated by applying forces to the calibration points with gauged weights between 0 and 100 g in 10 g increments. Each weight is applied five times ($n = 5$). The same forces

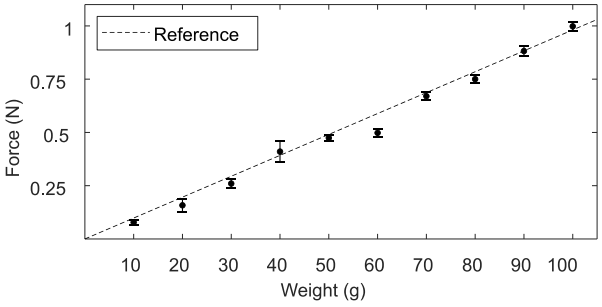

Figure 6: Average measured forces and standard deviation at the calibration point for various weight impacts over five trials.

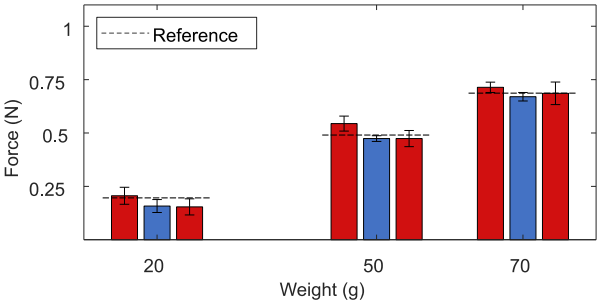

Figure 7: Average measured forces and standard deviation at evaluation points 1 (left, red) and 2 (right, red) in comparison to the calibration point (blue) for three weight impacts.

were applied in normal direction to the surface to two additional evaluation points to evaluate measuring accuracy at locations of the sensor that deviate about 5 mm from the calibration point to either side, as shown in Figure 5.

3 Results and Discussion

The results for the sensor's measuring accuracy are illustrated in Figure 6. The average absolute measuring error across all weights at the calibration point is 28 mN with a standard deviation of ±10 mN. In comparison, Figure 7 shows the mean measured forces at the two evaluation points. Over both evaluation points, an average measuring error of 25 mN with a standard deviation of ±9 mN is observed. The average response time between applied weight and force prediction of the sensor is approximately 500 ms.

The measurement accuracy at the calibration point indicates that the sensor allows sufficiently precise measurements for specific locations in the phantom that can be calibrated beforehand. In close proximity to the calibration point at a distance of 5 mm around it, measuring accuracy appears similar.

The performance when measuring at the evaluation points suggests that the sensor is able to determine impacts also quantitatively outside the calibrated areas. However, more remotely located evaluation points, the influence of the intended area, and simultaneous impacts are yet to be investigated. Localization of the impact within one sensor unit's surface is currently not possible. Furthermore, a response time of 500 ms may limit online feedback for some applications.

4 Conclusion

This work investigates a facile tactile sensor made from piezoresistive Velostat that can be integrated into soft and hard medical phantoms with the primary goal of creating affordable platforms for the preclinical investigation of soft articulated robots and for training surgical procedures with quantitative feedback. The highly integrated sensor can be arranged flexibly on a surface of interest, for example, the inner wall of the aorta, to measure and locate forces. The limitations of the current prototype are the inability to measure forces continuously instead of identifying extrema and the need for detailed calibration to acquire quantitative force measurements. The complete sensor surface appears sensitive when initially calibrated at one single point. Thus, one sensor strip can cover a large area of the phantom. A spatial resolution however for impacts within the surface area cannot be provided yet. A combination of several smaller sensor strips may address this challenge in the future. Further investigation shall deal with an extensive evaluation of the entire sensing surface, optimized sensor shapes and patterns as well as the transferability of one calibration point on one sensor to other sensors in the same phantom. Future work requires evaluation with experienced clinicians to create various interventional scenarios to further investigate on the sensor's limitations and validate the identified benefits. Integration and evaluation of the sensors in a smart phantom vessel with a closed shape and soft vessel walls may be the next step in this endeavor.

Author Statement

Research funding: This work has been funded by the Klaus Tschira Stiftung gGmbH (CatHERA 00.021.2019). The authors state no conflict of interest.

References

[1] K. Mc Namara, H. Alzubaidi, and J. Keith Jackson, "Cardiovascular disease as a leading cause of death: how are pharmacists getting involved?," 2019, doi: 10.2147/IPRP.S133088.

[2] E. B. Mazomenos *et al.*, "A Survey on the Current Status and Future Challenges Towards Objective Skills Assessment in Endovascular Surgery," *J. Med. Robot. Res.*, vol. 01, no. 03, p. 1640010, 2016, doi: 10.1142/s2424905x16400109.

[3] L. Karstensen, T. Behr, T. P. Pusch, F. Mathis-Ullrich, and J. Stallkamp, "Autonomous guidewire navigation in a two dimensional vascular phantom," *Curr. Dir. Biomed. Eng.*, vol. 6, no. 1, pp. 1–4, 2020, doi: 10.1515/cdbme-2020-0007.

[4] S. Aggarwal, E. Choudhury, S. Ladha, P. Kapoor, and U. Kiran, "Simulation in cardiac catheterization laboratory: Need of the hour to improve the clinical skills," *Ann. Card. Anaesth.*, vol. 19, no. 3, pp. 521–526, 2016, doi: 10.4103/0971-9784.185548.

[5] B. A. Eslahpazir, J. Goldstone, M. T. Allemang, J. C. Wang, and V. S. Kashyap, "Principal considerations for the contemporary high-fidelity endovascular simulator design used in training and evaluation," *J. Vasc. Surg.*, vol. 59, no. 4, pp. 1154–1162, 2014, doi: 10.1016/j.jvs.2013.11.074.

[6] E. Jeong, J. Lee, and D. E. Kim, "Finger-gesture recognition glove using velostat (ICCAS 2011)," *Int. Conf. Control. Autom. Syst.*, no. Iccas, pp. 206–210, 2011.

[7] M. Carrozzino, G. Avveduto, F. Tecchia, P. Gurevich, and B. Cohen, "Navigating immersive virtual environments through a foot controller," *Proc. ACM Symp. Virtual Real. Softw. Technol. VRST*, pp. 23–26, 2014, doi: 10.1145/2671015.2671121.

[8] D. Giovanelli and E. Farella, "Force Sensing Resistor and Evaluation of Technology for Wearable Body Pressure Sensing," *J. Sensors*, vol. 2016, 2016, doi: 10.1155/2016/9391850.

[9] B. W. Lee and H. Shin, "Feasibility Study of Sitting Posture Monitoring Based on Piezoresistive Conductive Film-Based Flexible Force Sensor," *IEEE Sens. J.*, vol. 16, no. 1, pp. 15–16, 2016, doi: 10.1109/JSEN.2015.2480600.

[10] D. A. Valle-Lopera, A. F. Castaño-Franco, J. Gallego-Londoño, and A. M. Hernández-Valdivieso, "Test and fabrication of piezoresistive sensors for contact pressure measurement," *Rev. Fac. Ing.*, vol. 2017, no. 82, pp. 47–52, 2017, doi: 10.17533/udea.redin.n82a06.

[11] M. Hopkins, R. Vaidyanathan, and A. H. McGregor, "Examination of the Performance Characteristics of Velostat as an In-Socket Pressure Sensor," *IEEE Sens. J.*, vol. 20, no. 13, pp. 6992–7000, 2020, doi: 10.1109/JSEN.2020.2978431.

[12] T. V. Papakostas, J. Lima, and M. Lowe, "A Large Area Force Sensor for Smart Skin Applications," *Proc. IEEE Sensors*, vol. 1, no. 2, pp. 1620–1624, 2002, doi: 10.1109/icsens.2002.1037366.